

# Time-reversed optical focusing through scattering media by digital full phase and amplitude recovery using a single phase-only SLM

Qiang Yang\*, Xinzhu Sang and Daxiong Xu  
*State Key Laboratory of Information Photonics and Optical Communications  
Beijing University of Posts and Telecommunications  
Beijing 100876, P. R. China  
\*yangqiang16@gmail.com*

Received 17 March 2014

Accepted 2 June 2014

Published 9 July 2014

Focusing light through scattering media beyond the ballistic regime is a challenging task in biomedical optical imaging. This challenge can be overcome by wavefront shaping technique, in which a time-reversed (TR) wavefront of scattered light is generated to suppress the scattering. In previous TR optical focusing experiments, a phase-only spatial light modulator (SLM) has been typically used to control the wavefront of incident light. Unfortunately, although the phase information is reconstructed by the phase-only SLM, the amplitude information is lost, resulting in decreased peak-to-background ratio (PBR) of optical focusing in the TR wavefront reconstruction. A new method of TR optical focusing through scattering media is proposed here, which numerically reconstructs the full phase and amplitude of a simulated scattered light field by using a single phase-only SLM. Simulation results and the proposed optical setup show that the time-reversal of a fully developed speckle field can be digitally implemented with both phase and amplitude recovery, affording a way to improve the performance of light focusing through scattering media.

*Keywords:* Tissue optics; phase retrieval; time-reversed optical focusing; optical phase conjugation; Gerchberg–Saxton algorithm.

## 1. Introduction

In scattering media, where light is strongly diffused, direct optical focusing beyond one optical transport mean free path ( $\sim 1$  mm for human skin) becomes infeasible. To overcome scattering, wavefront shaping techniques have been developed to achieve light focusing behind or inside a scattering layer. In these techniques, a spatial light modulator (SLM) is

used to shape the incident wavefront so that the maximal optical energy can be concentrated onto a specific point through (or inside) a scattering sample. Three kinds of methods have been developed to shape the optical wavefront: wavefront optimization with feedback signals, transmission matrix characterization, and time-reversal of the light through optical phase conjugation.<sup>1</sup>

This is an Open Access article published by World Scientific Publishing Company. It is distributed under the terms of the Creative Commons Attribution 3.0 (CC-BY) License. Further distribution of this work is permitted, provided the original work is properly cited.

Among these methods, the time-reversed (TR) optical focusing technique is directly based on the fact that the wave equation is time-symmetric in non-dissipative media. Therefore, for every wave diverging from a point light source, there exists in theory a second wave, the TR wave, which precisely retraces all its original paths in reverse order and converges in synchrony at the original point source, as if time were running backward.<sup>1</sup> Because of the time-symmetry, the TR wave eliminates wave distortions or scattering to achieve optical focusing at the original point light source, even in an inhomogeneous medium where the light waves are strongly reflected, refracted, or scattered.

The TR optical wavefront can be obtained from four-wave mixing (or holography) in nonlinear media,<sup>2</sup> or from phase conjugation by digitally controlled SLM.<sup>3</sup> Since both the phases of the original wave and the wave propagation direction are reversed, these media are called phase conjugated mirrors (PCMs).

In previous TR optical focusing systems, a programmable phase-only SLM<sup>4–6</sup> was adopted as the digital PCM that focused light through scattering media. In these schemes, only the phase, not the amplitude of the light, was modulated by the SLM. Because most of the signal information is contained in the phase terms, phase modulation is more essential than amplitude modulation. Still, controlling both the amplitude and phase of light is desired, since the additional control of amplitude provides a means of increasing the PBR of optical focusing for improved system performance.<sup>7</sup>

A seemingly feasible approach to achieve full amplitude modulation in the TR system is to use a single SLM which can modulate amplitude and phase independently and simultaneously. However, although phase-only and amplitude-only SLMs are commercially available, it is very difficult to find a single SLM which can accurately control both amplitude and phase independently. The difficulty is that the phase modulation of a SLM is coupled with the polarization angle changes of the incident light, which will change the amplitude (which dependently relies on the polarization angle) in the polarization-sensitive setup. An alternative way to modulate both the phase and amplitude of light is to combine a phase-only SLM with an amplitude-only SLM. In this scheme, two SLMs are placed in a very precisely designed setup, which demands that one panel's pixels to be quite accurately mapped

with those on the other panel. Furthermore, the amplitude-only SLM decreases the efficiency of output light by putting a polarizer in front. In a word, this two-SLM combined scheme is expensive and difficult to align.

To address these problems of both phase and amplitude reconstruction using digital SLMs, a new method is proposed in this work, which promises that time-reversing the wavefront of a fully-developed speckle field (with both phase and amplitude) is possible by using only a single phase-only SLM. In this method, a reflective phase-only SLM is divided into two panels which forms a pair of Fourier planes in the optical path. First, we simulated the speckle field behind a diffuser under coherent illumination. Then, to time-reverse the wavefront, one panel of the SLM was used as the PCM for phase reconstruction; another panel, displaying a phase pattern retrieved from the iterative Gerchberg–Saxton (G–S) algorithm, reconstructed the wanted amplitude at the plane of the PCM.

The simulation showed that the phase pattern retrieved through 6803 iterations reconstructed the wanted amplitude pattern with 2% error, if that phase pattern is illuminated by a coherent collimated reading beam. This is the first time, to our best knowledge, that the TR wavefront (with both amplitude and phase recovery) of a speckle field using just one phase-only SLM, has been demonstrated in simulation. Based on this, a proposed TR optical focusing setup with both phase and amplitude reconstruction is presented for potential experimental applications.

Apart from TR optical focusing, this method can be applied to all kinds of wavefront shaping techniques which use a programmable SLM to control both phase and amplitude of light in various applications, such as holographic display, laser beam forming, optical tweezer, and image delivery through scattering media.

## 2. Methodology

Here we demonstrate how to numerically reconstruct both amplitude and phase of a fully developed scattering light in a double diffraction process, and propose an experimental setup to focus light through scattering media.

In Sec. 2.1, a schematic diagram describes the principle of both amplitude and phase recovery in

the double diffraction process. Two phase-only SLMs are combined together, one for amplitude reconstruction by using G–S algorithm and the other for phase reconstruction, such that the TR light with both amplitude and phase can be achieved.

Based on the principle in Sec. 2.1, we proposed a practical TR optical focusing experimental setup using a single phase-only SLM in Sec. 2.2. In this proposal, a reflective SLM is divided into two panels which are combined together in a double diffraction process conducted in series. The advantages of using this single reflective SLM are discussed.

### 2.1. Employing G–S algorithm for both phase and amplitude reconstruction of the wavefront in speckle field

The standard G–S algorithm is normally used to retrieve the phase profile at two different parallel planes in a propagating optical field, given that the amplitude distributions in both planes are known.<sup>8</sup> Since the two parallel planes are usually a pair of Fourier planes, the G–S algorithm can be considered as a sort of iterative Fourier transformation algorithms (IFTAs).<sup>9</sup> Besides its original purpose, the G–S algorithm has been extensively used for creating computer-generated holograms (CGHs),<sup>10</sup> which are designed to numerically reconstruct the desired patterns at the CGH’s Fourier plane. Due to the CGH’s ability to recover complex shapes of

varied patterns, the G–S algorithm has been widely used in varied applications such as optical tweezers and laser beam forming.<sup>11</sup> In such applications, the G–S algorithm iteratively Fourier transforms the light propagation between the plane of computed hologram and its Fourier plane, where the desired pattern is supposed to be. In the meantime, a specific constraint (for example, the desired pattern of an optical tweezers, or the desired shape of an output laser beam) is added at any plane to confine the output pattern. In this work, we demonstrated that, besides these applications, the G–S algorithm can also be used in the numerical wavefront reconstruction of a fully developed optical speckle field. Figure 1 schematizes both phase and amplitude reconstruction of a speckle field by the G–S algorithm.

Two transmissive phase-only SLMs are placed separately at P1 and P2, composing a pair of Fourier planes which are essential for the Fourier transform in the G–S algorithm. In the wavefront reconstructing step, while the coherent plane-wave reading beam reads out the computed phase hologram  $\phi(x, y)$  at P1, the amplitude  $|E_0(u, v)|$  measured (or simulated) in the wavefront recording step can be reconstructed at P2, accompanied by an additional unwanted phase  $\psi_i(u, v)$ .

To retrieve the phase  $\phi(x, y)$  which numerically reconstructs  $|E_0(u, v)|$ , the iterative Fourier transforms are carried out in the process of G–S algorithm, as shown in Fig. 2.

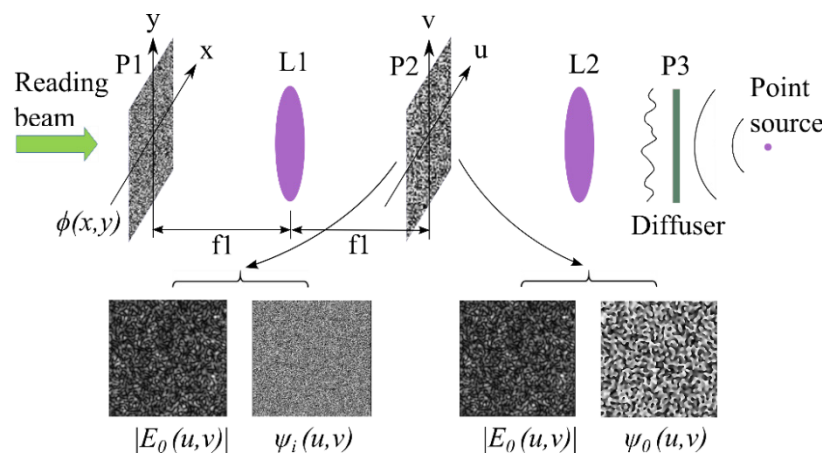


Fig. 1. Schematics of the G–S algorithm for the generation of a phase hologram to reconstruct the speckle field. P1 and P2 are a pair of Fourier planes with regard to the lens L1 whose focal length is  $f_l$ . P3 is the surface plane of the diffuser. Two steps are included here. First, in the wavefront recording step, the diffuser is illuminated by a coherent point source, and the diffuse light is collected by lens L2. The amplitude  $|E_0(u, v)|$  and phase  $\psi_0(u, v)$  at the plane P2 can be measured or simulated. After that, in the wavefront reconstructing step, the G–S algorithm is carried out numerically to retrieve the pure phase profile  $\phi(x, y)$  displayed at the plane P1, which reproduces the amplitude  $|E_0(u, v)|$  and an additional phase  $\psi_i(u, v)$  at the plane P2, while a coherent plane-wave reading beam reads out the computed phase hologram  $\phi(x, y)$ .

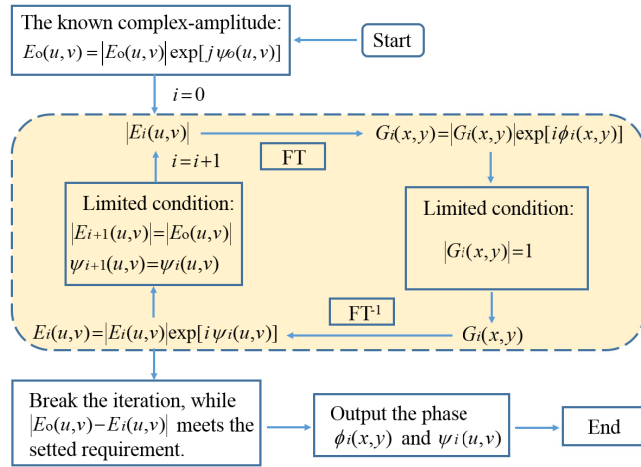


Fig. 2. Iterative process of G-S algorithm. FT and FT<sup>-1</sup> represent Fourier and inverse Fourier transform separately.

Inside the dashed box, the iterative Fourier transform is started from the known amplitude  $|E_o(u, v)|$ . The constraint  $|G_i(x, y)| = 1$  is set to provide a uniform amplitude distribution to  $G_i(x, y)$ , i.e., to limit  $G_i(x, y)$  to a phase-only profile before the next transform. After inversely Fourier transforming the modified  $G_i(x, y)$  with a uniform amplitude profile to obtain its Fourier pair  $E_i(u, v)$ , another constraint is carried out in each round of iterations, replacing the amplitude  $|E_i(u, v)|$  by  $|E_o(u, v)|$  while remaining the phase  $\psi_i(u, v)$ . Thus, a pure phase hologram  $\phi_i(x, y)$  (written as  $\phi(x, y)$  in Fig. 1) at P1, which generates the amplitude  $|E_o(u, v)|$  and an additional phase  $\psi_i(u, v)$  at P1's Fourier plane P2 under coherent illumination of a plane wave, is obtained in the end of iterations.

If  $\phi_i(x, y)$  and  $\psi_o(u, v) - \psi_i(u, v)$  are separately applied at the planes of P1 and P2 as shown in Fig. 1, the additional phase  $\psi_i(u, v)$  generated by  $\phi_i(x, y)$  will be compensated, then a full reconstruction with both phase and amplitude recovery at the P2 plane (acting as a PCM without the loss of amplitude) is achieved, resulting in a TR wavefront. This TR light can be used to suppress the scattering of the turbid media, such that an optical focusing at the original light source can be obtained.

## 2.2. Proposed optical setup for TR optical focusing through scattering media by using a single phase-only SLM

Based on the discussion in Sec. 2.1, a setup for TR optical focusing through scattering media is proposed for discussion,<sup>11</sup> as shown in Fig. 3. Different from the preliminary sketch using two phase-only modulators in Fig. 1, in this proposed setup, a single reflective phase-only SLM is used and divided into two panels (P1 and P2) for amplitude reconstruction and phase reconstruction separately. P1 and P2 are placed right in the conjugate focal planes of the virtual complex lens comprised by two lens (L1), and are read out in series by the coherent plane-wave reading beam. Unlike the two homonymic planes in Fig. 1, P1 and P2 shown in this section are two reflective planes. Furthermore, a wavefront recording sub-system is introduced in the proposed setup.

Compared with the demonstrative scheme using two transmissive SLMs in Fig. 1, using a reflective SLM based on liquid crystal on silicon (LCoS)

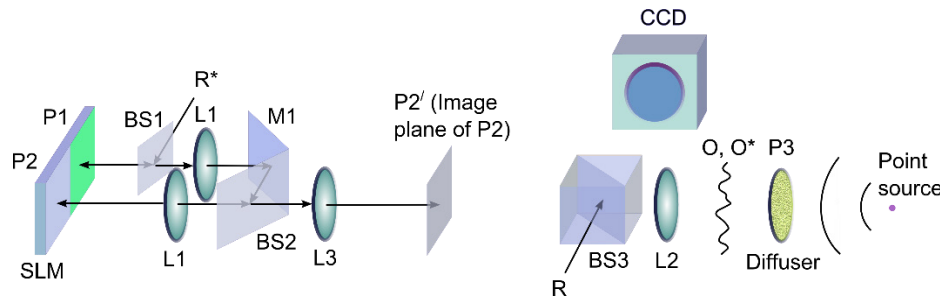


Fig. 3. Proposed optical setup for TR optical focusing through scattering media. O, the object light; O\*, the TR object light; R, the reference beam; R\*, the conjugated reference beam (reading beam); L, lens; P1 and P2, two identical panels of the SLM; M, mirror; BS, beam splitter. The phase-only SLM is divided into two equivalent panels P1 and P2, which are read out by R\* in series. The two identical lenses L1 compose a new complex virtual lens L, whose focal length is equal to half of the optical path between P1 and P2, such that P1 and P2 are the conjugate focal planes of each other. L1 is combined with L3, to compose an imaging system in which P2' is the image plane of P2 (and vice versa), while the magnification ratio precisely matches the ratio between the pixel size of the SLM and CCD.

technique has advantages such as lower cost, higher fill factor (less dead space between pixels increases light throughput and improves image quality), and smaller pixel size (higher spatial resolution).

In wavefront recording step, the amplitude and phase at the sensor plane of CCD can be easily measured experimentally at first, by using the standard phase-shifting holography.<sup>12</sup> Since the sensor plane of the CCD and the plane P2' are aligned to be rigorously symmetric with respect to the reflective surface of the beam splitter BS3, the object light's wavefront at these two planes are accurately equivalent, which means the light field (amplitude and phase) at P2' becomes known. The light field distribution at P2 can be derived from the one at P2' according to the magnification ratio of imaging lens array (L1 and L3), which precisely matches the size ratio between the SLM and the CCD's pixels.

In wavefront reconstructing step, to obtain optical focusing at the point source, a TR wavefront of the scattering light needed to be generated. First, while the reading beam reads out the phase hologram (retrieved by G-S algorithm) which is displayed on P1, the amplitude of light field accompanied by an additional unwanted phase is first reconstructed at P2. Second, if the appropriate phase pattern which compensates the addition phase is displayed at P2, the TR wavefront (with both amplitude and phase recovery) is then obtained at P2. After that, passing through the imaging lens assembly (L1, L3, and L2), the TR wavefront is achieved at P3. At last, while the TR object light O\* passes through the diffuser, a TR optical focusing can be achieved at the position of the original light source, by using this single phase-only SLM.

### 3. Simulation Results Based on the Proposed Setup

To prove the validity of schemes in Secs. 2.1 and 2.2, we need to verify at first if it is feasible to reconstruct a known speckle field's amplitude pattern from a phase pattern calculated by G-S algorithm, and then through the double diffraction process on SLM a TR wavefront of signal light with both amplitude and phase recovery can be achievable. In this section, first, we modeled the wavefront generated by an optical diffuser under coherent illumination and obtained the scattering field's phase and amplitude at a chosen plane. Then, G-S

algorithm is carried out to retrieve a phase pattern, which numerically reconstructed the amplitude at the chosen plane while the phase was read out by a plane wave. Finally, we analyzed the recovery error by comparing the reconstructed amplitude pattern with the known original pattern.

#### 3.1. Simulating the speckle field (with both phase and amplitude) behind a diffuser under coherent illumination

A speckle field with known phase and amplitude distribution, which can be achieved by simulation or experimental measurement, is needed to be obtained at first for reconstruction.

An optical diffuser, such as ground glass, scatters incident light randomly in directions without light absorption such that it is a simple model for simulating the speckle field. Diffuser is usually made of a transparent plate where grits of tens of micrometers in diameter are dispersed uniformly. Without any wavefront correction, images of a point source placed behind such a diffuser are totally distorted and cannot be distinguished.<sup>13</sup> In this work, to simulate the speckle field behind a diffuser in the wavefront recording step in Fig. 3, diffractive theory and Fourier transform were applied as below.<sup>14</sup>

In the paraxial approximation, diffraction theory reduces to a very simple and general formula:

$$E_{\text{out}}(r) = E_{\text{in}}(r) * h(r), \quad (1)$$

where  $E_{\text{in}}(r)$  and  $E_{\text{out}}(r)$  are the complex amplitudes of optical field in the input plane (P3) and output plane (P2') separately,  $h(r)$  is the impulse response of the diffraction system, and  $r$  represents the position at the respective planes using polar coordinates.

The convolution operation  $*$  can be transferred to Fourier domain according to convolution theorem, so that the image field  $E_{\text{out}}(r)$  is able to be simply computed by two Fast Fourier Transforms:

$$\begin{aligned} E_{\text{out}} &= FT^{-1}[FT(E_{\text{in}}) \cdot FT(h)] \\ &= FT^{-1}[FT(E_{\text{in}}) \cdot H], \end{aligned} \quad (2)$$

where  $H(\omega) = FT[h(r)]$  represents the coherent transfer function, and  $\omega$  is the spatial frequency of light.

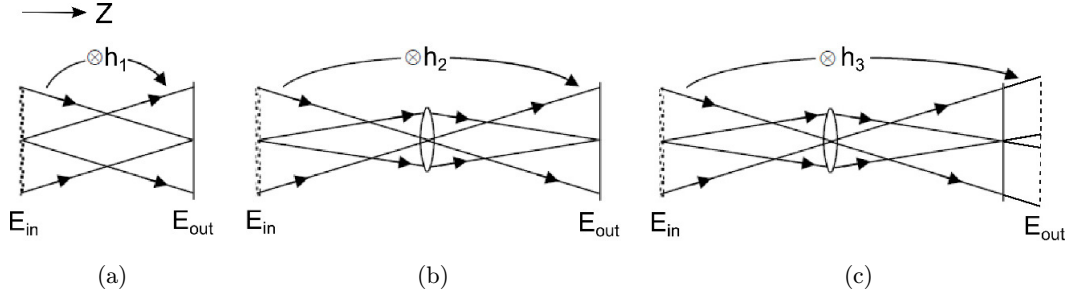


Fig. 4. The relationship of input field  $E_{in}$  and output field  $E_{out}$  under coherent illumination in paraxial approximation.  $E_{in}(r)$  and  $E_{out}(r)$  are separately corresponding to the complex amplitudes of optical field in the input plane (P3) and output plane (P2'), which are shown in Fig. 3. (a) Free space propagation model: No lens is used; (b) Focal plane model:  $E_{out}(r)$  is right at the image plane of  $E_{in}$ ; (c) Defocused plane model:  $E_{out}(r)$  is at the right side of the image plane of  $E_{in}$ .

In our case,  $E_{in}(r)$  represents the complex amplitude at the surface of the diffuser (P3) under coherent illumination by the point source. For the sake of simplicity, we will assume that the diffuser is a pure phase object:

$$E_{in}(r) = \exp[i\varphi(r)], \quad (3)$$

where the phase  $\varphi$  is uniformly distributed over a  $2\pi$  interval.

Three types of diffractive geometry were considered, all with a diffuser at the input plane (P3), and all assuming that light is propagated along the Z-axis for paraxial approximation.

In the free space propagation in Fig. 4(a), the impulse response of Fresnel diffraction is given by

$$h_1(r) = \frac{\exp(ikz)}{i\lambda z} \exp\left(i\frac{k}{2z}r^2\right), \quad (4)$$

$$H_1(\omega) = \exp(ikz) \cdot \exp(-i\pi\lambda z\omega^2),$$

where  $k$  is the wave number,  $z$  is the propagation distance of light in free space along the Z-axis, and  $\omega = \sin(\theta)/\lambda$ , where  $\theta$  represents the angle between the normal of the wavefront and the Z-axis.

In the focal plane model in Fig. 4(b), the impulse response of Fraunhofer diffraction is

$$h_2(r) = FT[cir(\rho)], \quad H_2(\omega) = cir(\rho), \quad (5)$$

where  $\rho$  denotes the diameter of the diffraction aperture.

In the defocused model in Fig. 4(c), two steps of diffractions are involved. First, the input field is imaged at the focal plane (shown by the solid line), corresponding to the Fraunhofer diffraction. Next, the optical field at the focal plane acts as the new input plane with respect to the defocused output plane such that the Fresnel diffraction in free space

propagation needs to be used. Combining these two steps, the impulse response of the whole system at the defocused plane can be described as

$$\begin{aligned} h_3(r) &= h_1(r) * h_2(r), \\ H_3(\omega) &= H_1(\omega) \cdot H_2(\omega). \end{aligned} \quad (6)$$

Since the defocused geometry has more generality, it was chosen for our numerical modeling. According to Eqs. (2), (3) and (6), the simulated complex amplitude of output optical field at the defocused plane in Fig. 4(c) is

$$E_{out}(r) = FT^{-1}\{FT[\exp(i\varphi(r))] \cdot H_3\}, \quad (7)$$

where  $E_{out}(r)$  is corresponding to the complex amplitude of speckle field at the plane of P2' in Fig. 3.

The simulated diffuser consists of  $512 \times 512$  micro phase-only modulators (or elements), which apply a random phase delay to the incident coherent wave. To control the speckle size in CCD's sensor plane, an aperture ( $512 \times 512$  elements) having a circular hole (whose diameter include 50

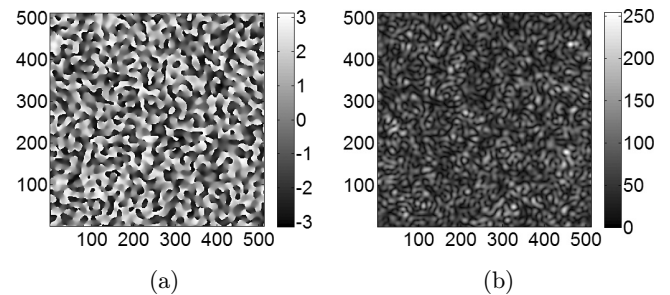


Fig. 5. The complex amplitude profile of a simulated fully-scattered speckle field at P2' plane in Fig. 3. (a) The phase profile at P2' plane. (b) The amplitude profile at P2' plane. The units of the gray bars are radians in (a), and the normalized standard grayscale in (b), respectively.

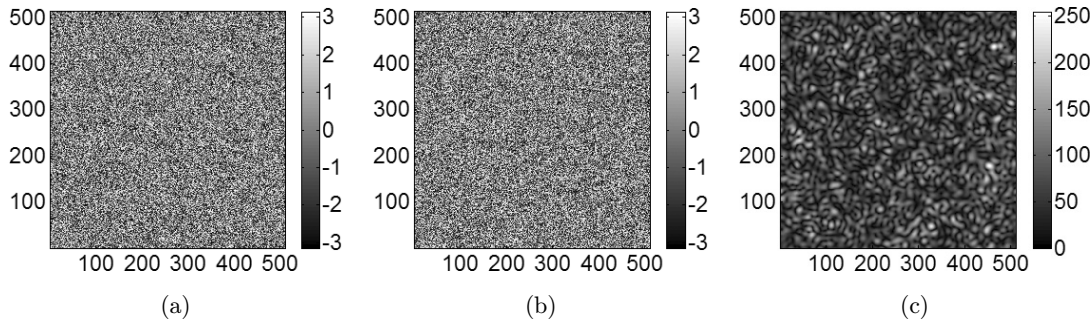


Fig. 6. The phase profile retrieved by G–S algorithm at P1 plane, and its diffractive field at its Fourier plane P2. P1 and P2 refer to the corresponding planes shown in Fig. 3. (a) The phase retrieved by the G–S algorithm at P1 plane. (b) The phase at P2 plane by Fourier transforming the phase in (a). (c) The amplitude at P2 plane by Fourier transforming the phase in (a). The units of the gray bars are radians in (a) and (b), and the normalized standard grayscale in (c).

elements, but can be adjusted as required) in its center, is put closed to the diffuser in this simulation. Each element of the aperture has the same size of the micro modulator of the diffuser, which is normally tens of micrometers. The coherent light's wavelength was set to be  $\lambda = 532$  nm. In the defocused geometry in Fig. 3, the distance between P3 plane and L2 (focal length is 3 cm) is 6 cm while P2' plane is 7 cm away from L2. That means, the P2' plane is 1 cm away from the image plane of P3, resulting in  $z = 1$  cm in free space propagation after the Fraunhofer diffraction.

After setting these parameters, the simulated phase and amplitude items of  $E_{\text{out}}(r)$  were then extracted from Eq. (7), and presented in Fig. 5.

### 3.2. Numerically generating the TR wavefront of the simulated speckle field in the proposed setup

In the proposed setup for TR optical focusing in Fig. 3, the P1 and P2 planes precisely form a pair of Fourier planes, such that the iterative Fourier transforms can be executed in the G–S algorithm. Based on the simulated results in Fig. 5, the phase displayed at P1 plane was retrieved by using G–S algorithm and shown in Fig. 6(a). Note that the simulated results in Fig. 5 have been rescaled by the magnification ratio between SLM and CCD, and transformed from P2' to P2 without tortuosity.

In the wavefront reconstructing step of the proposed scheme, the retrieved phase at P1 is read out by a coherent plane wave, resulting in a diffractive field at P2 plane as shown in Figs. 6(b) and 6(c). To achieve these results, 6803 iterations of Fourier

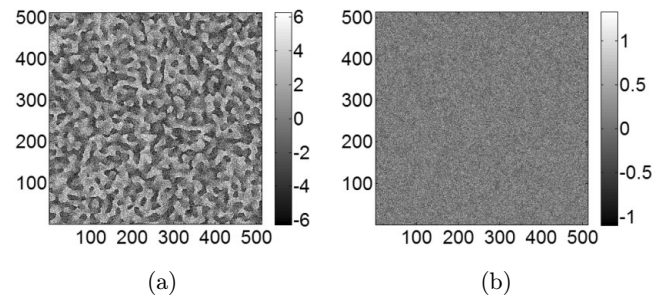


Fig. 7. The phase profile (a) displayed at P2 plane, and the amplitude error (b) at the same plane. The amplitude error was calculated by subtracting Fig. 6(c) from Fig. 5(b). The units of the gray bars are radians in (a), and the un-normalized grayscale in (b), respectively.

transforms as well as inverse Fourier transforms were executed.

While the desired amplitude in Fig. 6(c) was generated at P2 plane, an additional phase was also produced unwantedly at P2, while the calculated phase displayed at P1 plane was illuminated by the coherent plane wave. To accurately reconstruct the complex amplitude (with both amplitude and phase) of the speckle field at P2, a phase pattern aimed to compensate the additional phase produced by P1 was displayed at P2, as shown in Fig. 7(a). The error analysis of the reconstructed amplitude was also carried out as shown in Fig. 7(b), to evaluate the performance of wavefront reconstruction by using G–S algorithm.

## 4. Discussion and Summary

In the TR optical focusing technique, reconstructing both the amplitude and phase of a speckle field

offers a way to increase the PBR of optical focusing, which in theory is  $\sim 27\%$  higher than the scheme of simplex phase conjugation losing amplitude info.<sup>7</sup>

In this work, a new method of TR optical focusing method is proposed, which numerically reconstructs the full phase and amplitude information of a simulated scattered light field in a double diffraction process by using a single SLM. The diffraction theory in paraxial approximation is used to simulate the speckle field behind a diffuser with  $512 \times 512$  phase elements, while the G-S algorithm is adopted to retrieve the phase to reconstruct the amplitude of the speckle field if the phase pattern is illuminated by a plane-wave reading beam. According to the proposed optical setup and the simulation results, it is clear that the wavefront reconstruction (with both phase and amplitude) of a fully scattered optical field is entirely possible, using only a single phase-only SLM. The SLM is divided into two phase-only panels for amplitude reconstruction and phase reconstruction separately, which is feasible for the commercial phase-only SLMs (such as PLUTO, Holoeye, Germany) with a length-width ratio up to  $\sim 2$ . The reconstruction error of the recovered amplitude is controllable, since a customized break condition is applied in the algorithm loop. The total time for phase retrieval with a 2% amplitude reconstruction error is  $\sim 400.3$  s (with an Intel Core i5 3210M, 4 GB memory, and Intel Graphics 4000) for one simulation (without averaging), and can be greatly shortened by using a faster processor, such as a dedicated graphics processing unit (GPU). To estimate how the computational effort scales with the employed resolution of the diffuser, we also tried different resolutions of  $64 \times 64$ ,  $128 \times 128$ ,  $256 \times 256$ ,  $512 \times 512$  in simulations, and found that the corresponding iteration times (2286, 4581, 4966, 5226) increased, but not as much as the corresponding consumed time (4.8, 18.4, 80.3, 336.7 s). Both the iteration times and the consumed time are the averaged results taken from five simulations for each employed resolution. These results show, compared with the iteration times, that the computational amount in each Fourier transform is more sensitive to the employed resolution. Moreover, in the wavefront reconstruction process in experiment, there are some factors affecting the performance of TR optical focusing, such as the phase error in optical phase conjugation, the sample's lateral shift and the tilt of TR wavefront, which have been discussed in Refs. 4, 7 and 15. Compared

with the setup in Ref. 11, the proposed setup in Fig. 3 includes 5 passes of the readout beam through beam splitters, which significantly reduces the readout beam intensity. However, our proposed setup has a merit that the collimated readout beam is perpendicular to the panel of SLM, which does not disrupt the accuracy of the TR wavefront while the setup in Ref. 11 does.

The reconstructed TR wavefront is expected to trace back to the original light source and obtain an optical focusing, even after passing through a scattering medium such as a diffuser. The presented scheme can be applied in further experiments on optical focusing inside scattering media, such as the recently developed TR ultrasonically encoded (TRUE) optical focusing technique, in which the ultrasonically encoded light is used as a virtual coherent light source<sup>7,16</sup> for hologram recording.

## Acknowledgment

This work is partly supported by the National Science Foundation of China (61177018), the Program for New Century Excellent Talents in University (NECT-11-0596), and Beijing Nova Program (2011066).

## References

1. A. P. Mosk *et al.*, "Controlling waves in space and time for imaging and focusing in complex media," *Nat. Photonics* **6**(5), 283–292 (2012).
2. G. Lerosey *et al.*, "Time reversal of electromagnetic waves," *Phys. Rev. Lett.* **92**(19), 193904 (2004).
3. D. A. Miller, "Time reversal of optical pulses by four-wave mixing," *Opt. Lett.* **5**(7), 300–302 (1980).
4. M. Cui, C. H. Yang, "Implementation of a digital optical phase conjugation system and its application to study the robustness of turbidity suppression by phase conjugation," *Opt. Express* **18**(4), 3444–3455 (2010).
5. I. M. Vellekoop, M. Cui, C. H. Yang, "Digital optical phase conjugation of fluorescence in turbid tissue," *Appl. Phys. Lett.* **101**(8), 081108 (2012).
6. T. R. Hillman *et al.*, "Digital optical phase conjugation for delivering two-dimensional images through turbid media," *Sci. Rep.* **3**, 1909 (2013).
7. Y. M. Wang *et al.*, "Deep-tissue focal fluorescence imaging with digitally time-reversed ultrasound-encoded light," *Nat. Commun.* **3**, 928 (2012).
8. R. W. Gerchberg, W. O. Saxton, "A practical algorithm for the determination of phase from image



- and diffraction plane pictures,” *Optik* **35**, 227–246 (1972).
9. O. Ripoll, V. Kettunen, H. P. Herzig, “Review of iterative Fourier-transform algorithms for beam shaping applications,” *Opt. Eng.* **43**(11), 2549–2556 (2004).
  10. T. Dresel, M. Beyerlein, J. Schwider, “Design and fabrication of computer-generated beam-shaping holograms,” *Appl. Opt.* **35**(23), 4615–4621 (1996).
  11. A. Jesacher *et al.*, “Full phase and amplitude control of holographic optical tweezers with high efficiency,” *Opt. Express* **16**(7), 4479–4486 (2008).
  12. I. Yamaguchi, T. Zhang, “Phase-shifting digital holography,” *Opt. Lett.* **22**(16), 1268–1270 (1997).
  13. O. Katz, E. Small, Y. Silberberg, “Looking around corners and through thin turbid layers in real time with scattered incoherent light,” *Nat. Photonics* **6**, 549–553 (2012).
  14. S. Equis, P. Jacquot, “Simulation of speckle complex amplitude: Advocating the linear model,” *Proc. SPIE* **6341**, 634138-1–6 (2006).
  15. C.-L. Hsieh *et al.*, “Imaging through turbid layers by scanning the phase conjugated second harmonic radiation from a nanoparticle,” *Opt. Express* **18**(20), 20723–20731 (2010).
  16. X. Xu, H. Liu, L. V. Wang, “Time-reversed ultrasonically encoded optical focusing into scattering media,” *Nat. Photonics* **5**(3), 154–157 (2011).